High Power Diode Laser Marking and Engraving of Building Materials

L. Li*, J. Lawrence* and J.T. Spencer**

* Manufacturing Division, Department of Mechanical Engineering, UMIST, Manchester M60 1QD, UK.
** Company Research Laboratory, BNFL, Springfield Works, Preston, Lancashire, PR4 OXJ, UK.

ABSTRACT

A Diomed 60W-cw high power diode laser (HPDL) has been used for the marking and engraving of various building materials, including; marble, granite, clay tiles, ceramic tiles, roof tiles, ordinary Portland cement (OPC) and clay bricks. Morphological and microstructural characteristics are presented. The basic mechanisms of marking/engraving and characteristics of the beam absorption are described. The effects of material texture, colour and laser processing parameters are reported. The work shows that engraving depths of over 2mm (0.75mm for a single pass) can be achieved on marble substrates by thermal disintegration of $CaCO_3$ into loose CaO powder and CO_2 gas. Uniform amorphous glazed lines (1-3mm line width) of a colour different from the untreated materials can be generated on clay tiles, ceramic tiles, roof tiles, clay bricks and OPC by solidification phase formation after laser melting of these materials. Effects of atmospheric conditions, for instance using O_2 and Ar gas shrouds, have been examined, with different coloured marks being observed when different shroud gases are used. To demonstrate the practical worth of the process a UMIST crest has been marked on a ceramic tile using the system. Laser beam reflectivity is found to depend not only on material composition but also its colour. Reflectivity has been found to range between 12% to 18% for the various construction materials used in the experiment, except for marble (grey) which showed over 27% reflectivity. Since the HPDL is a portable device, in-field application of these processing techniques can be realised, which would be either impossible or difficult when using other types of lasers.

1. INTRODUCTION

Concrete, bricks, natural stones (such as marble and granite) and ceramic tiles are widely used in modern and traditional buildings, as well as in civil engineering structures and cemeteries. Even today, the overwhelming majority of natural stone and construction material marking/engraving is carried out using long established techniques. On-site marking/engraving is often performed using the traditional masonry tools of hammers and chisels, whilst in some instances pneumatic tools that utilise water-based solutions containing abrasive particles are used. Multiple production of relatively small scale items is carried out in jobshops using CNC machine tools incorporating high carbon steel or diamond engraving tools. For most stone mason's work the engraving process requires at least three stages including mark out, chiselling and finishing. Such work is not only laborious and time consuming but requires special skills and experience usually acquired over many years. Because stone and ceramic materials are hard and brittle, using mechanical means for marking and engraving is very likely to produce defects especially working on polished and hard surfaces. A small error may result in irreparable damage to the whole work. Extensive tool wear can also affect the quality, in terms of line width, depth and straightness, and repeatability of the work.

Despite the fact that laser marking techniques were established and characterised some time ago [1-3], to date only a limited number of studies have been conducted to determine the feasibility and the effects of laser marking/engraving natural stones and other construction materials. Most research has concentrated on the laser cutting and glazing of concrete and reinforced concrete using CO_2 and Nd:YAG lasers [4-9], most predominantly with regard to nuclear plant decommissioning. In order to make use of laser treated (glazed) concrete pieces for panelling and other decorative functions, a number of workers have studied the structural, physical and mechanical changes within the composition of concrete containing zeolite [10-11] and zirconia [12] resulting from surface exposure to CO_2 laser radiation. Of the published research that has been conducted using natural stone, almost all has been concerned with the cutting [13-15] and engraving [16] of marble using CO_2 lasers. Indeed, the engraving of large scale drawings (1.0m x 1.5m) using a CO_2 laser engraving device with computerised image pre-processing has been demonstrated [17]. Only a limited amount of work has concentrated on the processing of other natural stones, namely 'Jerusalem Rock' and granite [18]. Using an ion argon laser

[19] and a Nd:YAG laser [20] the indelible marking of ceramic materials through the irradiation and subsequent discoloration of the oxide layer of certain pre-placed coatings has been demonstrated.

Although it has been found that when processing hard rock (>1400 kg/m^3), laser radiation can be several times more effective than conventional mechanical tools due to excessive wear of the tools [18], and that laser processing offers higher productivity and greater design flexibility benefits [16-18], the commercial applications of such laser systems for the marking/engraving of natural stones and construction materials has been held in check by the non-portable nature of the lasers themselves. This is due either to the bulky auxiliary equipment, beam delivery optics, chiller units, etc., or the high operating power requirements (usually three-phase) of the lasers.

The high power diode laser (HPDL), is not only a truly portable laser, with the complete optical fibre system, having similar dimensions to a PC deck and weighing less than 20 kg, whilst only requiring a single-phase 240V power supply but, despite the current relatively low power levels of commercially available systems (60W-cw), has the potential for marking/engraving a variety of natural stones and construction materials, as demonstrated in this paper. This is principally because the energy efficiency of the HPDL is much higher than that of other high power lasers (HPDL: 30-50%, CO_2: 10-15%, flash lamp pumped Nd:YAG: 0.5-2%, Excimer 0.1-0.5%). Because of the HPDL portability, the marking/engraving of memorial headstones, monuments and civic and public buildings are distinct possible application areas, with the HPDL being used as either a pre-masonry operation, or, to actually produced finished engraved articles, or just simply used to produce inexpensive, indelible decorative surface markings.

In this paper, the basic characteristics of marking and engraving of various building materials (marble, granite, ceramic tiles, concrete and brick) using a portable 60W optical fibre delivered HPDL operating in the continuous mode are described. Morphology, microstructure and phase formation of the laser treated materials and the heat effects have been investigated. CAD/CAM and CNC systems are used to produce artistic and architectural effects such as crests and emblems.

2. EXPERIMENTAL PROCEDURES

A Diomed60 HPDL (wavelength: 810nm ±20nm) was used for the experiment, operating in the continuos mode with rated optical powers ranging from 0-60W. The laser beam was delivered to the work area through a 4 meter long, 600μm core diameter optical fibre, the end of which is attached to a 2:1 focusing lens assembly mounted on the z-axis of a 3-axis CNC gantry table. In the experiment, various building materials were irradiated using the focused high order mode HPDL beam of 0.6mm to 2mm diameter under various shroud gas conditions (Ar and O_2), traverse speeds (0.5mm - 20mm/s) and laser powers (0-35W measured at the workpiece). Figure 1 shows the experimental set-up for the HPDL processing experiment. The laser treated samples were then sectioned using a diamond rimed cutting blade and examined using optical microscopy, SEM, EDAX and XRD. The artistic and architectural emblems were produced using a Virtual Gibbs CAD/CAM software package.

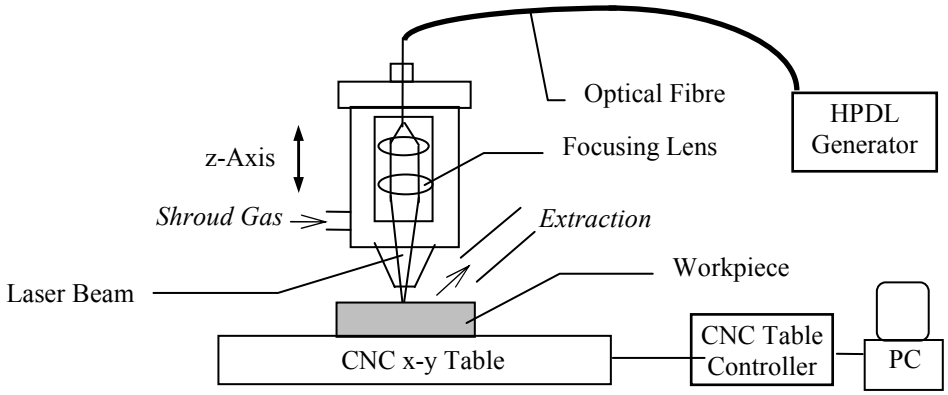

Figure 1: Schematic of the experimental set-up for the HPDL marking and engraving.

3. RESULTS

Using equally sized rectangular pieces of the natural stones and construction materials selected, 20 x 10 x 8 mm, experiments were carried out in order to examine the laser parameters and the morphological characteristics of the markings/engravings produced using the HPDL**.**

3.1 Minimum Laser Power Density Required to Initiate Marking And Engraving

By varying the HPDL power density within a series of discrete interaction times it was possible to determine the marking/engraving laser parameters for each material, in particular the minimum laser power density required to initiate surface melting. Table 1 summarises these findings.

Table 1: Minimum HPDL power density required to initiate surface melting under various interaction times.

HPDL Parameters	Materials						
	Marble	**Granite**	**OPC**	**Clay Brick**	**Clay Tile**	**Roof Tile**	**Ceramic Tile**
0.25 s, (W/cm^2)	-	-	2000	825	825	825	980
0.50 s, (W/cm^2)	2000	2000	1400	690	770	660	770
0.75 s, (W/cm^2)	1700	1800	1100	580	690	550	550
1.00 s, (W/cm^2)	1500	1700	1000	500	550	550	500
1.50 s, (W/cm^2)	1200	1450	960	420	500	550	480
2.00 s, (W/cm^2)	1200	1200	960	420	500	550	450
3.00 s, (W/cm^2)	1200	1000	960	420	500	550	450
4.00 s, (W/cm^2)	1200	1000	960	420	500	550	450

As Table 1 shows, a minimum energy density envelope for each material exists, below which it is not possible to initiate surface melting regardless of the interaction time.

3.2 Interaction of High Power Diode Laser With Selected Natural Stones and Construction Materials

With a fixed HPDL power density of 2 kW/cm^2 the beam was traversed once across the surfaces of the test pieces at a rate of 180 mm/min to create a single track. Two tracks were marked on the surface of each test piece, one using Ar as the shield gas whilst the other used O_2. Table 2 details the main constituents of the materials and the results of the laser interaction.

Table 2: Main material compositional constituents and the resultant HPDL marked/engraved track characteristics.

Building Materials	Main Compositional Constituents	Results				
		Colour	**Depth (mm)**	**Width (mm)**	**HAZ (mm)**	**Morphology**
Marble	$CaCO_3$	White for both O_2 & Ar.	O_2: 0.33 Ar: 0.38	O_2: 0.70 Ar: 0.64	O_2: 0.17 Ar: 0.17	Crystalline CaO with both O_2 & Ar.
Granite	SiO_2	Black for both O_2 & Ar.	O_2: 0.68 Ar: 0.71	O_2: 1.28 Ar: 1.28	O_2: 0.01 Ar: 0.01	Cracks & porosities with both O_2 & Ar.
Roof Tile	SiO^2, Al_2O_3, CaO	Very light green for both O_2 & Ar.	O_2: 0.60 Ar: 0.60	O_2: 1.63 Ar: 1.65	O_2: 0.17 Ar: 0.17	Cracks & many porosities with O_2 & Ar.
OPC	CaO, SiO_2	Light green. O_2 gave darker green.	O_2: 0.82 Ar: 0.79	O_2: 1.84 Ar: 1.75	O_2: 0.20 Ar: 0.16	Cracks & porosities. More cracks with Ar.
Clay Brick	SiO_2, Al_2O_3,	Dark blue. O_2 gave darker blue.	O_2: 0.50 Ar: 0.50	O_2: 1.58 Ar: 1.58	O_2: 0.30 Ar: 0.30	Few cracks. Porosities only with Ar.
Clay Tile	SiO_2, Al_2O_3	Dark blue/black. O_2 gave darker colour.	O_2: 0.55 Ar: 0.57	O_2: 1.54 Ar: 1.57	O_2: 0.38 Ar: 0.36	Cracks & porosities with both O_2 & Ar.
Ceramic Tile	SiO_2, Al_2O_3	Dark green. O_2 gave darker green	O_2: 0.80 Ar: 0.80	O_2: 1.50 Ar: 1.50	O_2: 0.20 Ar: 0.24	Few cracks & porosities. Large porosities with Ar.

As Table 2 shows, HPDL interaction on all but the marble sample resulted in the creation of a continuous, undulating vitreous surface of various colours ranging in thickness from 0.50 mm on the clay brick, to 0.82 mm on the concrete. Glazing of these materials is made possible simply by the fact that their composition consists mainly of the glass forming elements SiO_2 and Al_2O_3, and in varying amounts, the glass network modifying

elements of Mg and Fe_2O_3. As such, on rapid localised heating from the HPDL beam rapid localised melting of the elements within the composition is initiated and on solidification a vitreous glaze is formed.

From a cross-sectional analysis of the vitrified glazed tracks, the formation of 'knife-edge' porosity in the glazes was clearly discernible (Figure 2). This is presumed to be caused by excessive CO_2 gas pressure rupturing the walls of large bubbles within the molten glass that are released during heating [11]. Such knife-edge porosities were observed to be a common feature particularly on the granite, brick and concrete samples. This is due to the fact that the composition of these samples contain very little of the glass network modifying elements that reduce the viscosity of the molten glass and thus allow gas bubbles to escape. In contrast, because of their composition, knife-edge porosities were less evident on the clay and the ceramic tile samples.

(a) (b)

Figure 2 : Cross-sectional SEM images of the vitreous glazes produced on (a) granite and (b) clay tile with an O_2 shield gas.

Additional forms of porosity were also observed in the vitreous glazes of the concrete and roof tile samples. This is due to the substantial presence within their composition of Ca (60-70wt%), especially in the form of $Ca(OH)_2$, which is not vitrifiable.

(a) (b)

Figure 3: Optical micrograph of the vitreous glazed surface of (a) clay brick and (b) granite with an O_2 shield gas.

As Table 1 and Figure 3(a) show, surface microcracking of the vitreous glazes was generally not a feature on the majority of samples. This is due principally to the good thermal characteristics of the materials which allow the efficient dissipation of heat away from the surface into the bulk of the material, thus preventing the generation of a steep thermal gradient. However, as Figure 3(b) shows, large cracks were microscopically observed in the vitreous glaze of the granite sample. This is probably due to the solidified vitreous material over-contracting on

cooling as a result of the elevated melting temperature caused by the high SiO_2 content (approximately 90wt%) of the granite.

A cross-sectional analysis of the glazed vitreous surface of the samples revealed clearly the presence of a heat affected zone (HAZ) surrounding the vitrified layer. Figure 4 shows the HAZ observable around the glazed layer of the clay brick. Typically the HAZ was relatively small, ranging in thickness from 0.17 mm on the clay tile to 0.30 mm on the concrete around the glazed layer, with the HAZ surrounding the marble mark/engraving being approximately 0.4 mm. However, the HAZ on the granite sample was measured to be an almost negligible 0.01 mm. In the instance of all the materials except for the granite, the HAZ is the result of the breaking down of the $CaCO_3$ with material's composition which occurs at temperatures between 825^{o}C and 950 ^{o}C, resulting in CaO. In the case of granite, the HAZ is quite simply a region of semi-glazed SiO_2 resulting from the surface heat dissipation.

(a) (b)

Figure 4: Cross-sectional optical micrograph showing the HAZ for (a) clay brick and (b) granite. Both glazes generated using O_2 as the shroud gas.

3.3 Effects of Different Shroud Gas Conditions on Marking

The type of shroud gas used has a number of effects besides influencing the vitreous glaze colour. Generally, whether using either Ar or O_2 as the shield gas, the vitrification of the constituent components of the material when incident with the HPDL beam results in a volume change, as Figure 5 clearly shows. However, for all the materials, the volume change is much increased when O_2 is used as the shield gas.

(a) (b)

Figure 5: Cross-sectional micrograph of clay brick showing the difference in volume change of the vitreous glaze when using (a) Ar as the shield gas and (b) O_2 as the shield gas.

Also, as Figure 6 shows, the quality of the surfaces, in terms of smoothness, porosity and microcracks, of the vitreous glazes produced is significantly influenced by the type of shield gas employed. The use of O_2 as the shield gas significantly reduces the number of porosities and microcracks within the vitreous glaze as well as producing a much smoother surface.

(a) (b)

Figure 6: Surface optical micrograph of vitreous glazed tracks on clay tile produced with (a) Ar shield gas and (b) O_2 gas shield.

3.4 High Power Diode Laser Marble Engraving

The interaction of the laser with marble tiles exhibited significant difference from that of other materials. Through careful selection of the HPDL operating parameters, principally power density and traverse speed, both the marking and engraving of marble was possible, as Figure 7 shows.

(a) (b)

Figure 7: Surface optical micrograph of marble showing, (a) marked tracks and (b) engraved track. Both using Ar as the shield gas.

Engraving to depths of up to 0.75 mm has been demonstrated, and as Figure 9(b) shows, the edges of the engravings are of a high quality. For marble, neither the edge quality or the engraving depth appear to be effected by the type of shield gas employed.

Because marble is a metamorphic rock composed of recrystallized calcite or dolomite, and as such the main component of marble (95wt%) is $CaCO_3$ limestone, there is very little SiO_2 or other glass forming elements within its composition. As such, when the marble is incident with a laser beam the rapid localised surface heating and melting does not result in the formation of a vitreous amorphous glaze, but instead results in the decomposition of the $CaCO_3$ at temperatures between 825^0C and 950^0C in accordance with the recognised chemical reaction [13-16];

$$CaCO_3 = CaO + CO_2 - 42.52 \text{ kcal/mole}$$

As one can see, the breakdown results in unslaked lime (CaO) and carbon dioxide gas (CO_2). The CO_2 gas simply enters into the atmosphere, whilst the CaO either rests in the irradiated zone producing a mark, or, if the power density is sufficiently high, is vaporised and ejected out of the irradiated zone.

Figure 8 shows a typical cross-section through an engraved marble track exposing the HAZ which surrounded the marking/engraving to a depth of approximately 0.3 mm. As mentioned previously, the HAZ is simply CaO, and in the case of marble is simply semi-unslaked lime resulting from heat dissipation from the surface.

Figure 8: Optical micrograph of a cross-section through a HPDL engraved track in marble using O_2 as the shield gas.

The natural occurrence in marble of white Ca rich veins and their effects on the HPDL interaction were investigated. As Figure 9 shows, these veins result in 100% reflection of the incident beam. To overcome this problem it was necessary to apply a black water based ink coating of less than 0.01 mm thickness to the surface in order to increase the absorption.

Figure 9: Surface optical micrograph of marble showing the effects of natural Ca rich white veins.

3.5 Practical Architectural Marking

To demonstrate the use of the laser system for practical marking and engraving, a UMIST crest was marked on a ceramic tile using the HPDL system (Figure 10). A dark green coloured mark was obtained on the back side (unglazed face) of the tile. The crest was plotted using a Virtual Gibbs CAD/CAM graphics package and transferred to the CNC controller. The laser head was automatically lifted upwards (thus defocusing the beam on the workpiece) when the marking of a single letter or symbol was complete such that clear separation was obtained.

Figure 10: A UMIST crest marked using the 3-axis CNC HPDL marking/engraving system.

4. DISCUSSION

4.1. Colour Change Mechanisms

For marking purposes, laser heating and melting does not always guarantee a colour change for marking purposes. For example, the laser melting of previously glazed surfaces of siliceous ceramic tiles does not generate a colour change since there is little or no phase changes involved. For such materials the application of additional colour pigments may be necessary for marking. However, for most non-metallic materials where surface glazing is not already present, a colour change by laser heating or melting always occurs. This is because most of these materials are either hydraulically bonded (like concrete and natural stones) or fired below their melting points (such as tiles and bricks), thus during the laser heating and melting processes, each mineral undergoes a characteristic set of changes. These may include a rearrangement of the crystal structure of existing minerals, for instance the α/β transition to quartz, the loss of water (thus the hydraulic bond) and the release of CO_2 and the development of new phases at high temperatures especially when melting commences. As Figure 11 shows, amorphous phases have been produced after the laser melting of granite, OPC, clay bricks clay tiles and ceramic tiles which were previously in crystalline structures. An example of this is shown in Figure 11 where an XRD analysis of ceramic tiles before and after HPDL marking clearly indicates the amorphous phase in the laser glazed area. Indeed, Figure 12 shows a high magnification SEM images of a section of untreated granite and of the amorphous vitrified glaze resulted from HPDL interaction. From Figure 12(a) the crystalline structure of the natural state granite is clearly visible whist in Figure 12(b) the very fine glass structure can be seen distinctly.

Although, the glazed areas are brittle and cracks and/or porosities were seen in almost all of the glazed area, they may not significantly affect the cosmetic effect of the permanent marking if viewed at a relatively short distance. Indeed, the contrast of colours produced without the use of any added colour pigments is sufficient to enable recognition at a distance. Intermediate phase changes at elevated temperatures below the melting point constitute the HAZ with less distinctive colour changes. Hydraulically bonded materials, such as the OPC, exhibited a relatively large HAZ since several phase changes occur across the whole range of temperature profile down to 200^0 C with the formation, for example, of CaO around 500^0 C, wollastonite and mullite at temperatures above 800^0 C etc.

The new phase formation not only alters the material properties, such as brittleness and density, but is also the principal reason for colour change. The observed dark blue colours (as seen on the siliceous bricks and the granite) and the green colours (as seen on the clay tiles), for example, are believed to be caused by the formation of Fe(II) oxidation phases whilst the red colour in the untreated materials is attributed to the presence of the Fe(III) oxidation state [21]. The use of O_2 as the shroud gas has, in most cases, resulted in a higher probability of Fe oxide formation and thus a darker glaze. The EDAX analysis of granite (Figure 13) showed an increase in O_2 content after laser glazing. Similar features were also seen in the other materials.

(a) (b)

Figure 11: XRD diagram showing a crystalline structure (a) before laser glazing and (b) an amorphous state after laser glazing for ceramic tiles.

(a) (b)

Figure 12: High magnification SEM images of (a) the untreated crystalline structure of granite and (b) the amorphous vitreous glazes produced by the HPDL.

(a) (b)

Figure 13: EDAX analysis of granite, unglazed area (a) and (b) laser glazed area.

4.2. Beam Absorption Characteristics

In order to understand the beam absorption characteristics of the HPDL with the construction materials, an experiment was conducted to determine the reflected laser power in comparison to the incident power when the samples were placed at 45 degrees to the incident laser beam. The results are shown in Figures 14 and 15, and indicate clearly that the dark coloured granite, clay brick, OPC the ceramic tiles and the clay tiles have an angular beam reflectivity in a range between 12% to 18%, whilst the marble (grey) showed over 27% reflectivity. In these tests melting had occurred for laser powers above 8W.

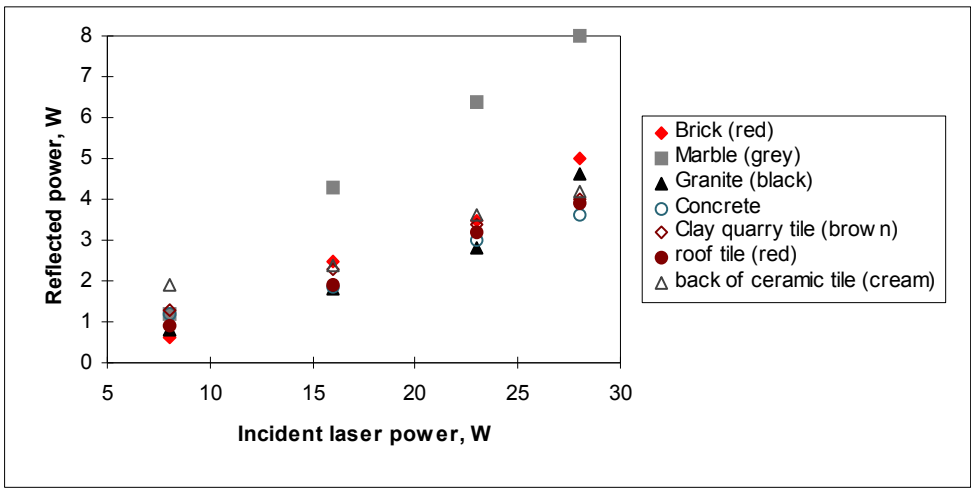

Figure 12: Reflection test results of various materials at different incident diode laser power levels.

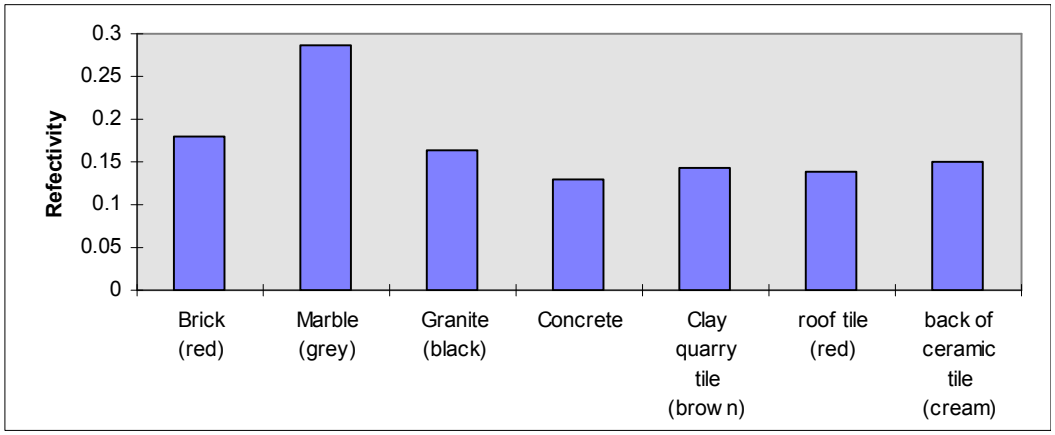

Figure 15: Angular reflectivity for various structural materials at 810nm wavelength.

The data in the above test were obtained by measuring the reflected power (45 degree to the workpiece surface) three times for each incident power level with an average being taken. The results may represent the lower limits of reflectivity of these materials since there may be certain amount of beam scattering in other directions not covered by the power meter (Power Wizard). The overall error of the above measurement may be in the range of 5 to 10 %. The results can be used to indicate relative reflectivity of these materials. For example, it can be seen from Figure 15 that concrete has the highest beam absorption whilst the grey coloured marble has the lowest beam absorption. The beam absorptivity of other materials studied appear to be very similar.

6. CONCLUSIONS

The characteristics and mechanisms of marking and engraving natural stone and ceramic materials using a HPDL have been investigated. It has been found that different shroud gases may have significant influences on the quality and colour of the marks generated, with the O_2 gas shroud giving less porous and darker coloured glazes (except for roof tiles) compared with those obtained when using Ar gas. The beam absorption of these materials is generally high, with angular reflectivity below 30%, but is, however, colour dependent, with light coloured materials reflecting more of laser beam Very low power (above 10W-cw) is needed to generate a glaze which changes the colour of the materials, although for engraving, much higher power levels (above 30W-cw) are required. The work has demonstrated clearly the feasibility of a potential portable flexible marking and engraving system using a HPDL.

ACKNOWLEDGEMENTS

The authors would like to express their gratitude to the EPSRC (Process Engineering Group, Grant No. GR/K99770 and CDP Group, CASE award No. 95562556), BNFL (Agreement No. A751688), Diomed Ltd., and the Nuffield Foundation (Ref: SCI/180/94/260/G) for their financial support to the project. Also, many thanks go to Carol Duckworth and Dave Goddard of BNFL, Springfield Works for sharing their time and expertise.

REFERENCES

1. Asmus, J.F., Scranlini, M., Zetler, M.J., (1976), "Rock Surface Texture Alterations Using Lasers", *Lithoclastia*, Jan. 1976, Vol 1, p 37.
2. Bernard, B., (1982), "Laser Marking Techniques", *Proceedings of ICALEO '82: Laser Materials Processing*, Sep. 1982, Boston, MA., Vol 31, p 14-16.
3. Klimt, B.H., (1988), "Review of Laser Marking and Engraving", *Lasers & Optronics*, Sep. 1988, Vol 7 **(9)**, p 61-67.
4. Sugita, K., Mori, M., Fujioka, T., (1986), "Applications of Laser for Cutting Concrete", *Concrete Engineering*, Sep. 1986, Vol 26 **(9)**, p 13-22.
5. Hamasaki, M., (1987), "Experimental Cutting of Biological Shield Concrete Using a Laser", *Proceedings of the International Symposium on Laser Processing*, May 1987, San Jose CA., Vol 852, p 68.
6. Yoshizawa, H., Wignaraja, S., Saito., H., (1989), "Study on Laser Cutting of Concrete", *Journal of Japan Welding Society*, April 1989, Vol 20 **(1)**, p 31-36.
7. Li, L., Modern, P., Steen, W.M., (1992), "Laser Fixing and Sealing of Radioactive Contamination on Concrete Surfaces", *Proceedings of LAMP '92: Science and Applications*, June 1992, Nagoaka, Japan, p 843-848.
8. Li, L., Modern, P., Steen, W.M., (1994), "Laser Surface Modification Techniques for Potential Decommissioning Applications", *Proceedings of RECOD '94*, April 1994, London, UK., p 427-440.
9. Li, L., (1994), "Laser Removal of Surface and Embedded Contamination on Construction Materials", in SPIE Proceedings, Vol. 2246, *Optics of Productivity in Manufacturing*, June 1994, p84-95
10. Sugimoto, K., Wignarajah, S., Nagasi, K., Yasu, S., Kimura, K., Kasuya, M., Kureha, S., (1992), "Fundamental Study on Laser Treatment of Architectural Materials", *Proceedings of ICALEO '90: Laser Materials Processing*, Nov. 1990, Boston, MA., Vol 71, p 302-312.
11. Wignarajah, S., Sugimoto, K., Nagai, K., (1992), "Effect of Laser Surface Treatment on the Physical Characteristics and Mechanical Behaviour of Cement Based Materials", *Proceedings of ICALEO '92: Laser Materials Processing*, Oct. 1992, Orlando, FL., Vol 75, p 383-392.
12. Borodina, T.I., Valyano, G.E., Ibragimov, N.I., Pakhomov, E.P., Romanov., A.I., Smirnova, L.G., Khabibulaev, P.K., (1991), "Examination of Changes in Oxide Ceramics in Melting the Surface With Laser Radiation", *Journal of Physics and Chemistry of Materials Treatment*, Sep. 1991, Vol 25 **(5)**, p 541-546.
13. Basov, N.G., Barkadse, V.N., Glotov, E.P., (1986), "Experimental Study of Laser Treatment of Marble", *Soviet Physics Doklady*, Feb. 1986, Vol 31 **(2)**, p 172-173.

14. Pires, M., Ferreira, A., Ribeiro, M., Teixeira, R., Rodrigues, C., (1988), "Marble Cutting by Laser", *Proceedings of SPIE: Laser Technologies in Industry*, Sep. 1988, San Jose, CA., Vol 925, p 622-625.
15. Kumar, M., Biswas, A.K., Sriniwas, K., Nath, A.K., (1995), "Marble Cutting With CW CO_2 Laser", *Proceedings of SPIE: Novel Applications of Lasers and Pulsed Power*, May 1995, San Jose, CA., Vol 2374, p 34-39.
16. Appelt, D., Cunha, A., (1988), "Cutting and Engraving of Materials With a CO_2 Laser", *Proceedings of SPIE: Laser Technologies in Industry*, Sep. 1988, San Jose, CA., Vol 925, p 618-621.
17. Zang, B., Su, B., Liu, Y., (1992), "Laser Engraving", *Proceedings of SPIE: Rapid Thermal and Laser Processing*, Nov. 1992, San Jose, CA., Vol 1804, p 138-143.
18. Gurvich, L., Yatsiv, S., Shachrai, A., (1992), "Rock Processing With CO_2 Laser Radiation", *Proceedings of SPIE: 8th Meeting on Optical Engineering in Israel*, May 1992, Tel-Aviv, Israel, Vol 625, p 297-305.
19. Alexander, D.R., Khlif, M.S., (1996), "Laser Marking Using Organo-Metallic Films", *Optics and Lasers in Engineering*, July 1996, Vol 25 **(1)**, p 55-70.
20. Herren, F., Hofmann, M., (1991), "Laser Marking of Ceramic Materials, Glazes, Glass-Ceramics and Glasses", *US Patent 5030551*, 9 July 1991.
21. Jackson, N., Dhir, R.K., (1992), *Civil Engineering Materials, 4th Edition*, Macmillan Press, New York, NY., p 393.